Computer simulation of a novel cycle helmet

Sheffield Hallam University
Faculty of health and wellbeing

Ashish John Stanley – 29029604
AshishJohn.J.Stanley@student.shu.ac.uk

Introduction:

Making learning to ride a safe experience increases the chances of kids continuing to ride cycles and reaping its benefits. Part of making the riding experience safe includes protective gear like helmets. The low usage of cycle helmets among kids has provided an area for promoting safer cycling habits (Teyhan, Cornish, Boyd, Joshi, & Macleod, 2016). Although studies report the effectiveness of awareness programs in increasing usage of bike helmets (Ederer, et al., 2016) (Farley, Haddad, & Brown). There is a considerable knowledge gap in what design and economic factors that make a bike helmet unfavourable in a parent's or kid's opinion.

Based on inputs received from interviews of parents and a market search of current bike helmets for kids, a helmet is design to cater to the needs of kids. Bike helmets are designed to protect and yet not drastically increase the energy spent by the rider for the sake protection. Hence a computational fluid dynamics (CFD) analysis is performed to study the aerodynamic effects on the helmet.

A large vertical of design and innovation in cycling is aimed at reducing the aerodynamic effects. Drag forces(F_d) acting against the cyclist influences the performance of the cyclist and is a function of coefficient of drag (Cd) and front surface area(A) (Crouch, Burton, LaBry, & Blair, 2017). [rho- density of air, U – velocity].

$$Fd = Cd.\frac{A\rho U^2}{2}$$

Bike helmet designs have evolved to provide minimal drag force. Simulation of aerodynamic forces have helped experiment and accelerate the process of designing and improving performance for biking helmets. This aim of the assignment is the design a cycling helmet for the target user group and conduct computational fluid dynamics (CFD) analysis on the model. The CFD analysis will be used to interpret the fluid dynamics effect the helmet model will have on the rider. These results will be compared with results of simulation of a bare head.

Literature Review:

Wind tunnel testing has been used widely to understand the aerodynamic forces on a rigid object (Souza & & Girardi, 2017). CFD simulations are reported to have a difference of 11% in results when using Reynolds-averaged Navier–Stokes (RANS) equations for simulation when compared to wind tunnel testing results in a aerodynamic study of cyclist positions (Defraeye & Hespel, 2010).

The RANS equations are computationally less costly and are not capable of capturing complex flow features and cannot resolve vortex shredding (Thé & & Yu, 2017). The simulation in the current assignment is run with a low velocity and due to the low Reynolds number would have issues accurately simulating in a turbulence model. Low Reynolds correction algorithm is proved to improve the accuracy of the model (Aftab, A., Rafie, Razak, & Ahmad, 2016).

CFD simulations are a representation of real-world phenomena and need to be optimized to provide the closest accurate representation. Using a convergence study to arrive at a mesh independent CFD simulation structure has been highlighted as verification procedure for CFD analysis. (Stern, Wilson, Coleman, & Paterson, 2001).

Computer Aided Design (CAD) Model:

Using SOLIDOWRKS a CAD geometry is modelled to the accommodate the desired features on the helmet. The CAD model of the helmet are dimensioned to fit the given CAD model of a head.

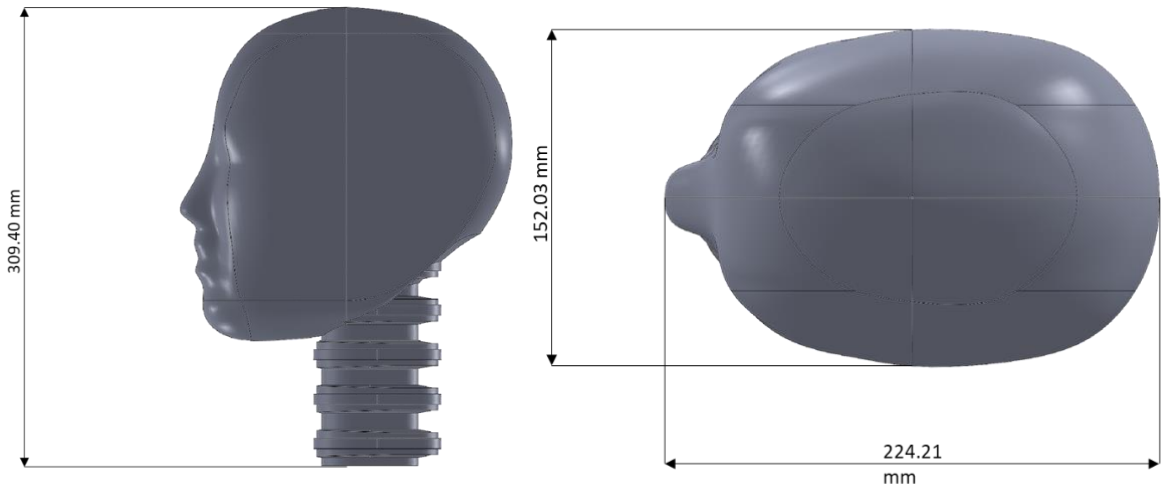

Figure 1 (a): Side view of head. (b) Top view of head

The helmet id designed keeping in my mind the insights provided by parents and the market study conducted. The features incorporated in the design are:

1) Covers a large surface area of the head. Has an extension to the back of the head to provide better protection.

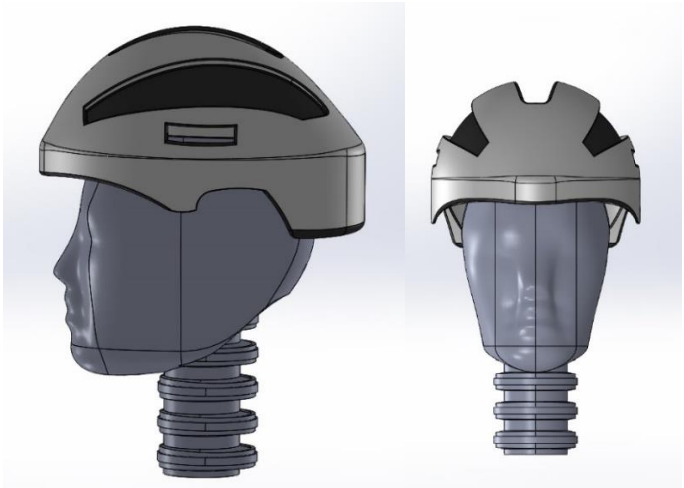

Figure 2 (a): Top view of the helmet. (b) Bottom up view of the helmet

2) A larger than head size cavity to accommodate for customizable padding to fit varied head sizes and provide protection.

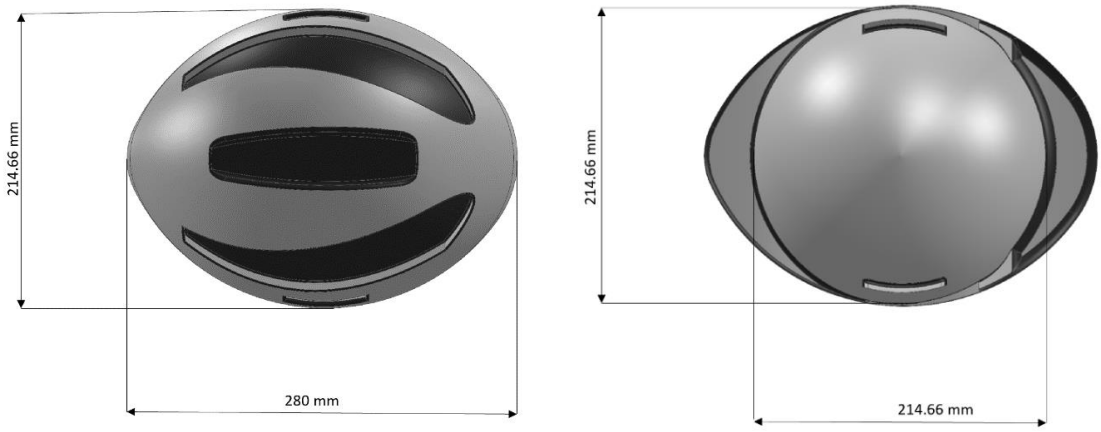

Figure 3(a): Top view of the helmet. (b) Bottom up view of the helmet

3) Thin walls at the side to remove weight from the model and prevent neck injuries due to a heavy helmet considering the padding would be added weight.

4) Two vents on the side to provide for cooling. Larger vents are not provided considering the end user does not typically spend long durations riding and rides in moderate weather conditions.

Pre-Processing for Computational Fluid Dynamics:

To simulate the aerodynamic forces acting on the helmet and head a wind tunnel is modelled using Workbench 2019 R2 (Chowdhury, Alam, & Mainwaring, 2011). Two regions are defined around the head and helmet geometry to allow for finer meshing to study the wake behaviour. The neck from the head geometry is removed to improve the quality of the mesh. The edges of the neck produced skeweed cells during meshing.

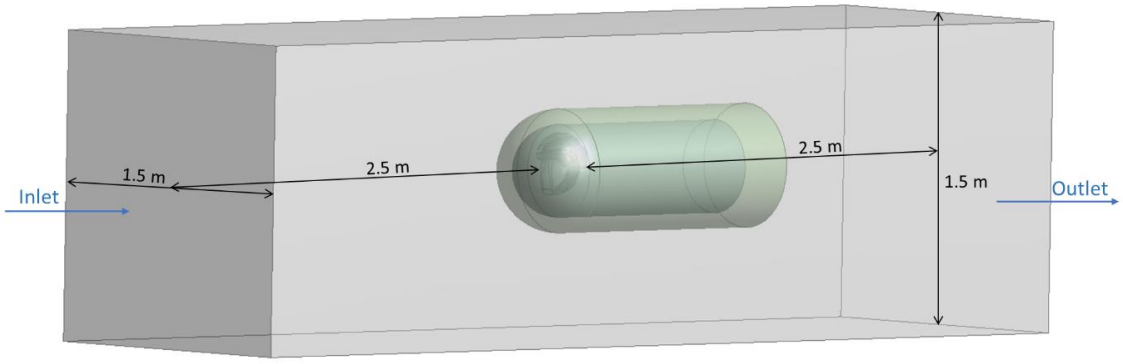

Figure 4: Geometry of wind tunnel with refinement regions for simulation

The head and helmet assembly are placed at a 0˚ yaw, 0 ˚ pitch and 0˚ roll without a sting. The wind tunnel simulation will run at a turbulence intensity (T_i) of 1% and turbulent viscosity ratio (T_{vr}) of 2. Wind speed of 3 m/s (Reynold Number=55,589) is used for the wind tunnel simulations to replicate the average speeds of kids cycling.

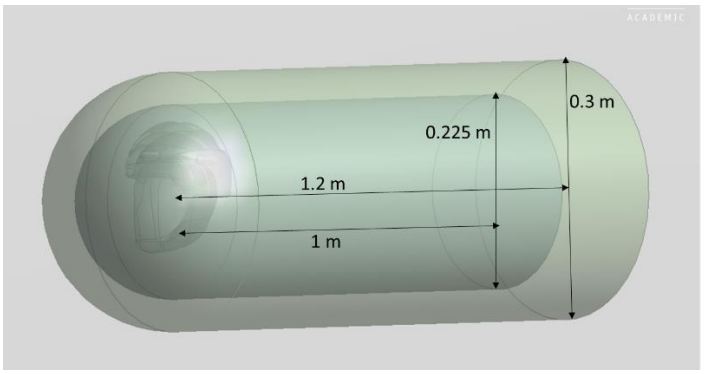

Figure 5: Dimensions of refinement regions in the wind tunnel

MESHING:

Using ANSYS Fluent 2019 R2 in meshing mode the multiple meshes were created to perform a convergence study for the head geometry without the helmet. The convergence study is performed to arrive at a mesh independent solution. Table 1 shows the results from the different meshes formed. From the convergence report the mesh with the least cells and within an acceptable change is used to run a simulation on the head and helmet assembly.

Mesh	Head Alone	Refinement Region1	Refinement Region2	Tunnel	Maximum Skewness	Cell Count (x 10^6)	Cd	Average Y+
A	3	6	9	200	0.781	2.19	0.273	2.316145
B	4	8	12	200	0.796	1.00	0.276	3.217518
C	5	10	15	200	0.775	0.56	0.279	3.808327
D	6	12	18	200	0.774	0.35	0.292	4.237252
E	8	16	24	200	0.744	0.18	0.333	4.72033

Table 1: Convergence report to find a mesh independent solution.

From the above table Mesh B is chosen. Mesh A has a Cd value of 0.273 and is twice more in cell count than Mesh B. We select Mesh B over C since the Average Y+ value is lower even though the Cd difference between Meshes A, B and Meshes B, C is the same.

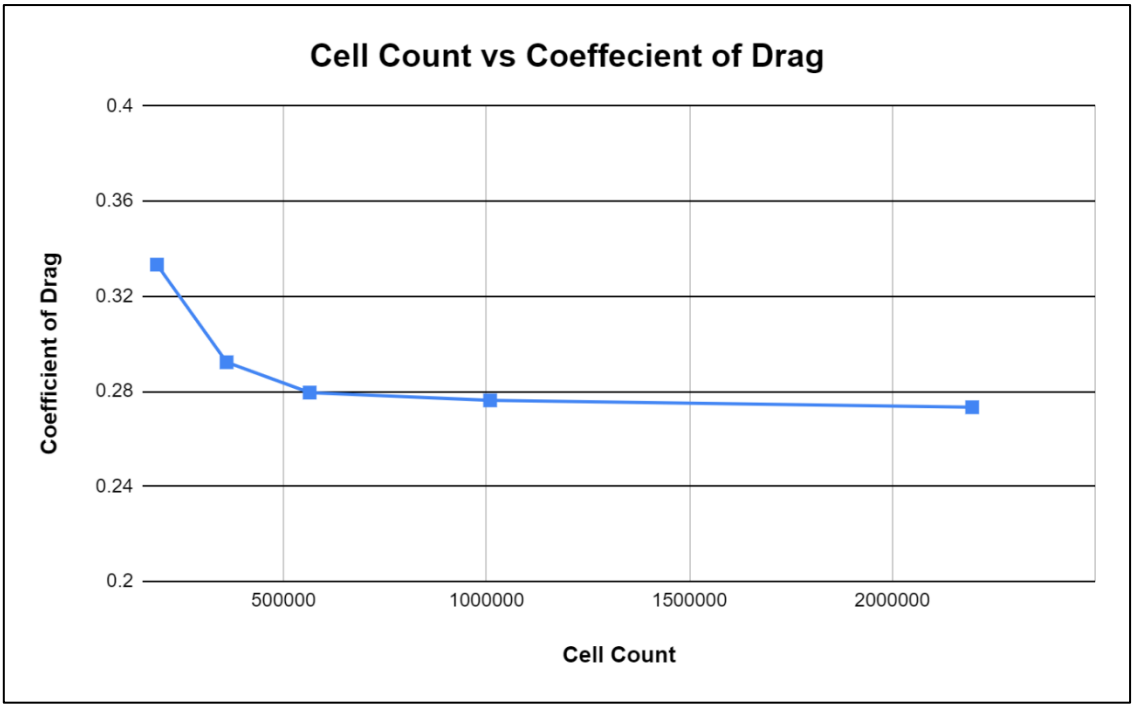

Figure 6: Plot showing Cd value for different mesh

The mesh is generated using polyhedral shaped structures. Polyhedral meshes showed an improvement in convergence speed and homogeneous wall sheer stresses (Spiegel, 2011). The final head and helmet geometry were simulated with the following mesh sizes at a growth rate of 1.2 . The mesh is finer in the refinement regions to capture more information around the model.

Region	**Cell Size**
Head and Helmet	4
Refinement Region 1	8
Refinement Region 2	12
Tunnel Walls	200

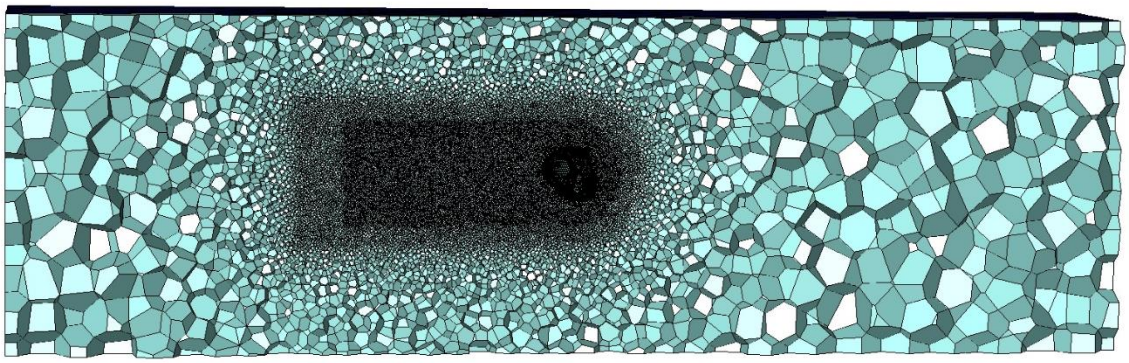

Figure 7: Mesh of bare head (10,09,066 cells)

Computational Fluid Dynamics:

The CFD analysis used a research licence of ANSYS Fluent 2019 R2. The study employs steady Reynolds-Averaged Navier–Stokes (RANS) equations using a k-ω shear stress transport (SST) model. The selected options for simulation are selected to achieve highest accuracy while keeping computational costs moderate and the solution robust.

Due to low computational costs and robustness RANS numerical equations are used. The RANS equations are a stable numerical method. It is less computational since it does not resolve individual eddy structures in the turbulent flow and just creates a single wake to represent the turbulent flow.

The low Reynolds number for the problem requires the usage of low Reynolds number correction algorithm to model the transition from laminar to turbulent flow better. (Cid Montoya, et al., 2018). The k- ω model does a better job compared to the k-epsilon model in resolving the near wall dynamics, this will better indicate the flow separation.

The prismatic layers are defined to accurately simulate the turbulence at the boundary layers. They are orthogonal prisms located near the boundary wall in the volumetric mesh. 5 prismatic layers are used for the computational setup. The Y+ value of the simulation gives an idea of how well the simulation captures the dynamics in the prismatic layers. A Y+ value less than 5 will mean we are in the viscous sublayer.

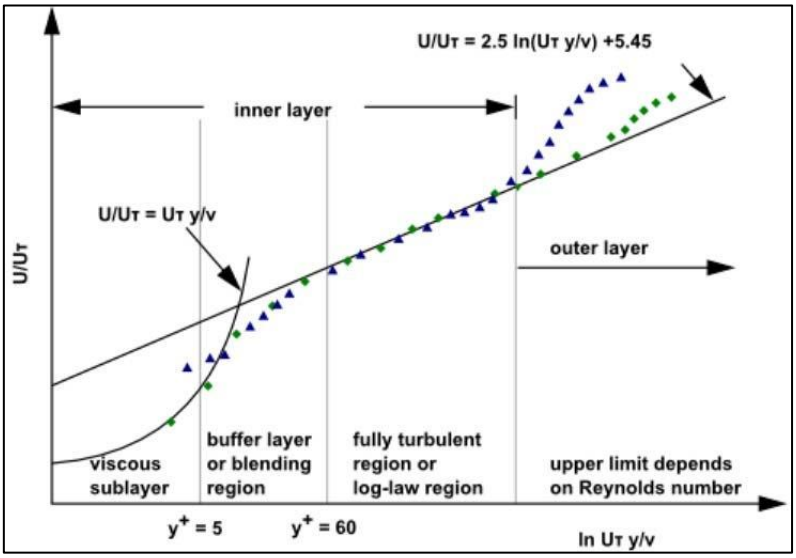

Figure 8: Subdivisions of boundary layer (Králik, (2016))

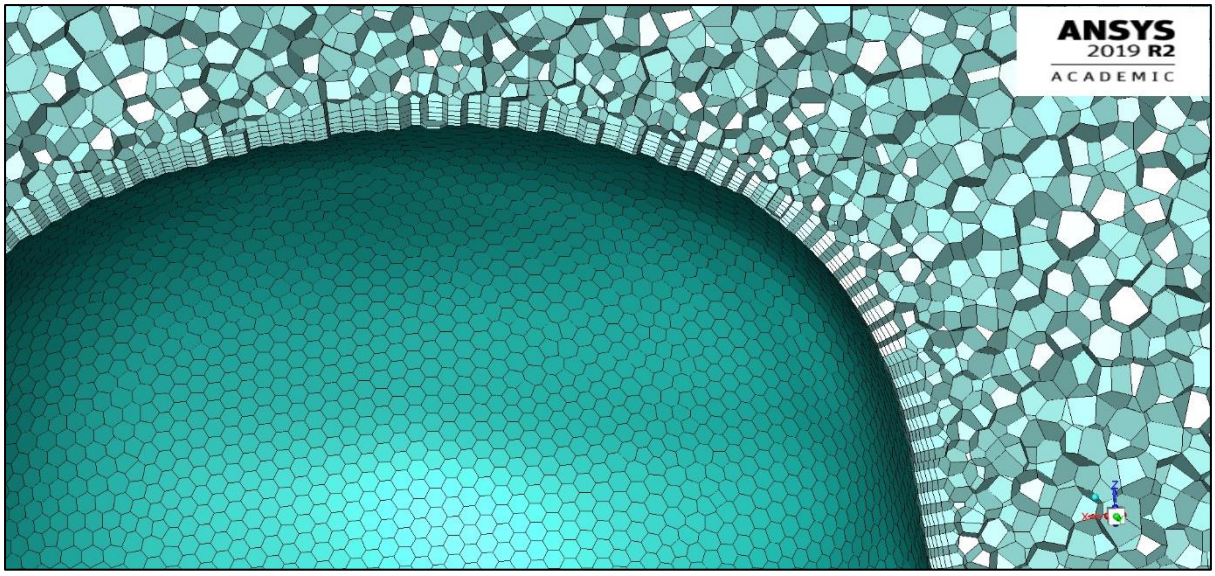

Figure 9: Close up view of the bare head mesh showing the defined prismatic layers.

A second order scheme is used to achieve higher accuracy although it takes harder for the solution to converge. The second order scheme uses more points of the mesh for the computation making it computationally costlier than the first order scheme. The simulation is run at steady state since the flow is time invariant.

The simulations are set to run for 1000 iterations or until convergence is achieved. Convergence is judges by not only looking as the scaled residuals but also looking at the coefficient of drag force. The criterion for residuals convergence was set to 10^{-4}. Below is the convergence shown by the residuals in the plot for the head and helmet geometry.

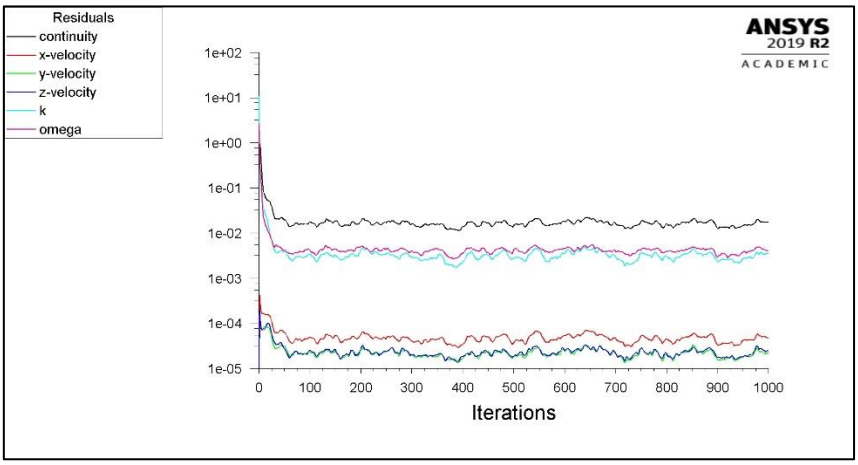

Figure 10: Plot showing the convergence of residuals for the CFD simulation of the head and helmet geometry.

Once the simulation is completed the coefficient of drag is calculated from the report file by calculating the average Cd value of all the iterations. Path lines and contours help visualise the fluid dynamics from the simulation.

Results:

Mesh	Bare Head /Head + Helmet (cell size)	Refinement Region1 (cell size)	Refinement Region2 (cell size)	Tunnel (cell size)	Maximum Skewness	Cell Count (x 10^6)	Cd	Average Y+
Bare Head	4	8	12	200	0.796	1.00	0.276	3.217518
Head and Helmet	4	8	12	200	0.843	1.34	0.406	1.905652

The table above shows the Cd value for the simulation of the bare helmet and that of the head and helmet.

Pressure Coefficient:

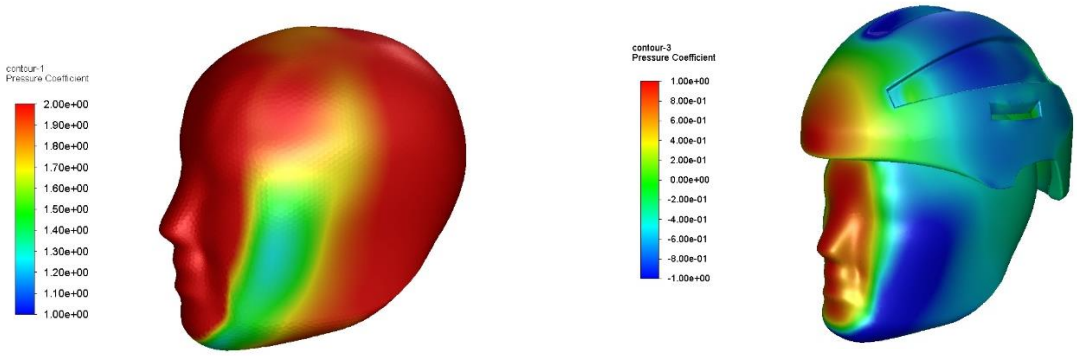

Figure 11: Pressure coefficient of bare head and bare head with helmet

The contours showing pressure coefficient can be seen to have a high stagnating pressure as soon as the air flow hits the cyclists face. The bare head contours do not have any negative pressure regions. A very early trip in the airflow is noticed in the bare head. The helmet on the other hand has a negative pressure indicating either turbulence in the regions of negative pressure.

Skin Friction:

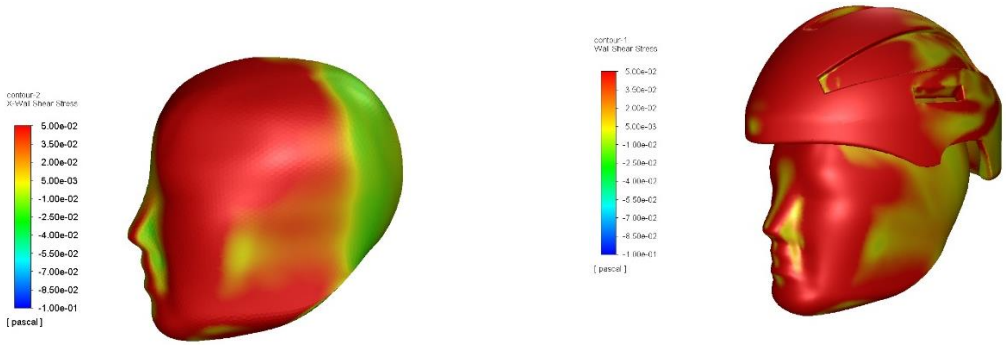

Figure 13: Sheer Stress of bare head and bare head with helmet

From the sheer stress contours, we can notice that the air flow in the head and helmet stays to the surface of the head for a large surface area. The small patch of low pressure in the bare head could indicate that there is high flow velocity since there is an indication of less skin friction as well in that region. This could suggest the flow starts to leave the surface layer. A clear flow separation can be seen in the head than in the helmet.

Velocity:

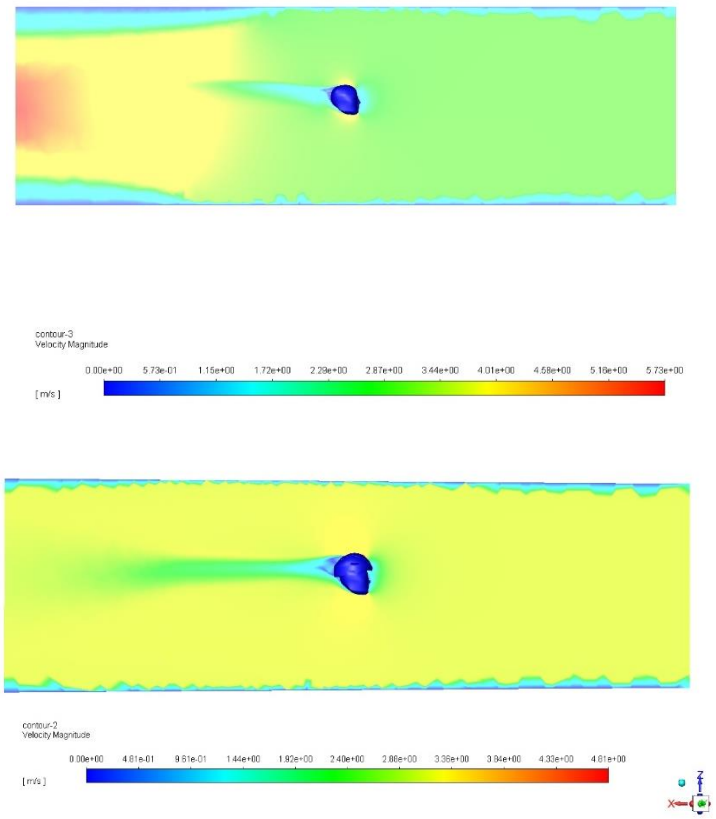

Figure 14: Velocity magnitude along a quadric plane on the y-axis.

From the velocity magnitude we can see a wake being formed. Right after the head a small region of low velocity magnitude is seen suggesting a turbulence in that region. The helmet creates a larger wake and hence we can say a larger turbulence is created. The wind tunnel outlet in the bare head shows some high velocity magnitude. This could cause interference.

Pathlines – Velocity Magnitude:

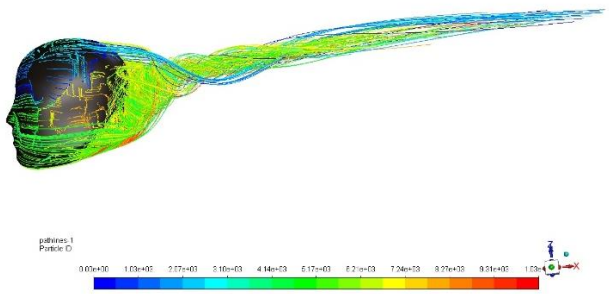

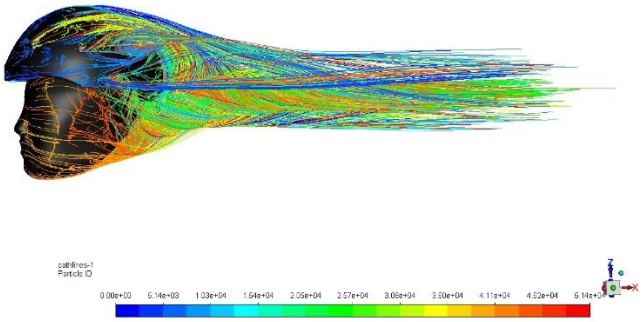

Figure 15: Velocity magnitude shown using path lines.

From the path lines we can identify that the path lines in the helmet are denser than those in the bare helmet. This suggests that the helmet has created more turbulence.

Flow separation from oil flow path lines:

The oil flow in the bare head shows a clear separation of the flow which coincides with the interpretation from the skin friction contours. In the helmet the air flow separation is hard to determine, the skin friction contours are a better indication for the air flow separation in case of the head. Certain regions of the helmet in the head and helmet model show flow separation though.

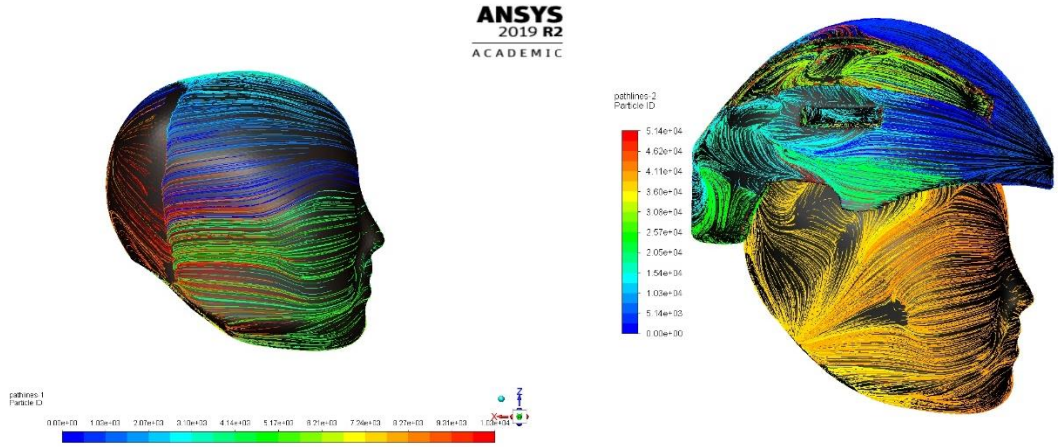

Figure 16: Oil flow path lines of velocity magnitude to show flow separation.

Critical Evaluation:

The helmet design has has a sherpical shaped area for the head to it. This can cause fit issues with vary head sizes. This problem was faced with the assembly of the head and helmet. While there was a small gap between the head and the helmet at the sides there was a large gap between the top of the head and helmet.

From the simualtion a fairly large difference in the coeffecient of drag is observed between the bare head and the head and helmet. This large increase in Cd (0.17) can be due to the large frontal surface area. The helmet is placed with a large distance to the head in the assemble to have clearence between the head and helmet. This increases the front surface area of the helmet. Fixing the clearence issue between the head and helmet can reduce the frontal area.The helmet does not have many vents, which further increases the frontal area and leads to increase in Coeffecient of drag.

Both the meshes have a Y+ value below 5. This ensures that the flow is resolved well in the boundry layer of the surface. An acceptable level of maximum skewness has been achieved for the meshes. This indicates the meshes are of good quality. The convergence study has ensured the mesh choosen makes the solution mesh independent.

The air flow sepertion is earlier in the helmet than in the bare head model. This could be due to the debossed features on the helmet causing the air flow to trip earlier and cause a turbulence. From figure 14 and figure 15 we can say that the helmet has a created a larger turbulence than the head.

The wake can be further resovled if we had a complex numerical method compared to RANS equations to resolve individual eddies. From figure 15 we can see a turbulence from the small vents of the helmet on the side. The wake is larger with the helmet behind the helmet. This shows the helmet has created a larger turbulence.

Conclusion:

The aerodynamics of the helmet has been compared with that of a bare head. Using K-Omega SST , Low Reynolds number calculation and RANS equations the flow has been simulated. The helmet has an increased drag force effect on the rider. (Cd Helmet and head = 0.406 , Cd Bare head = 0.276).

WORD COUNT: 2083 EXCLUDING TABLES AND REFERENCES

References

Aftab, S., A., M., Rafie, A. M., Razak, N. A., & Ahmad, K. A. (2016). Turbulence model selection for low Reynolds number flows. *PloS one*, 11(4).

Chowdhury, H., Alam, F., & Mainwaring, D. (2011). A full scale bicycle aerodynamics testing methodology. *Procedia Engineering*, 13, 94-99.

Cid Montoya, M., Nieto, F., Álvarez, A. J., Hernández, S., Jurado, J. Á., & Sánchez, R. (2018). Numerical simulations of the aerodynamic response of circular segments with different corner angles by means of 2D URANS. Impact of turbulence modeling approaches. . *Engineering Applications of Computational Fluid Mechanics,*, 12(1), 750-779.

Crouch, T. N., Burton, D., LaBry, Z. A., & Blair, K. B. (2017). Riding against the wind: a review of competition cycling aerodynamics. *Sports Engineering*, 20(2), 81-110.

Defraeye, T. B., & Hespel, P. &. (2010). Aerodynamic study of different cyclist positions: CFD analysis and full-scale wind-tunnel tests. *Journal of biomechanics*, 43(7), 1262-1268.

Ederer, D. J., Van Bui, T., Parker, E. M., Roehler, D. R., Sidik, M., Florian, M. J., & Ballesteros, M. F. (2016). Helmets for Kids: evaluation of a school-based helmet intervention in Cambodia. *Injury Prevention*, 22(1), 52-58.

Farley, C., Haddad, S., & Brown, B. (n.d.). The effects of a 4-year program promoting bicycle helmet use among children in Quebec. *American Journal of Public Health.*, 86(1), 46-51.

Králik, J. ((2016)). CFD Simulation of Air Flow Over an Object with Gable Roof, Revised with Y+ Approach. *Transactions of the VŠB–Technical University of Ostrava, Civil Engineering Series.*, 16(2), 85-94.

Souza, P. V., & & Girardi, D. (2017). Drag force in wind tunnels: A new method. . *Physica A: Statistical Mechanics and its Applications*, 467, 120-128.

Spiegel, M. R. (2011). Tetrahedral vs. polyhedral mesh size evaluation on flow velocity and wall shear stress for cerebral hemodynamic simulation. . *Computer methods in biomechanics and biomedical engineering*, 14(01), 9-22.

Stern, F., Wilson, R. V., Coleman, H. W., & Paterson, E. G. (2001). Comprehensive approach to verification and validation of CFD simulations—part 1: methodology and procedures. *J. Fluids Eng.*, 123(4), 793-802.

Teyhan, A., Cornish, R., Boyd, A., Joshi, M. S., & Macleod, J. (2016). The impact of cycle proficiency training on cycle-related behaviours and accidents in adolescence: findings from ALSPAC, a UK longitudinal cohort. *BMC public health*, 16(1), 469.

Thé, J., & & Yu, H. (2017). A critical review on the simulations of wind turbine aerodynamics focusing on hybrid RANS-LES methods. . *Energy*, 138, 257-289.